

# The status of the ESRF

Annick Ropert for the ESRF Project Group  
ESRF, BP 220  
F - 38043 Grenoble Cedex

## Abstract

Construction of the ESRF source started in 1988 as a joint project of European countries. The facility consists of a 200 MeV electron linear accelerator, a 6 GeV fast cycling booster synchrotron and a 6 GeV low emittance storage ring optimized to produce high brilliance X-rays from insertion devices. The project is now in its final assembly and testing phase, with the first beam injected in the storage ring scheduled in February 1992. A ten-month commissioning time is planned for the storage ring. From then on, the first set of beamlines will be installed. Routine operation for users will start in 1994.

This paper reviews the progress in installation and commissioning of the different components of the accelerator complex. Installation is proceeding in accordance with the sequential completion of the accelerator buildings. The electron linac reached design performance in the 1  $\mu$ s pulse operation in June 1991. The booster reached design specifications (5mA / 6 GeV / 10 Hz) in December 1991. Results of commissioning are reported. Finally the progress on procurement and installation of the different components of the storage ring is described. First tests with beam are to start at the very beginning of 1992.

## 1. INTRODUCTION

The European Synchrotron Radiation Facility is a third generation, insertion device oriented synchrotron light source. It is optimized to provide high brilliance X-rays in the  $\text{\AA}$  range, mostly from undulators and wigglers installed in a large number of straight sections.

The construction phase was launched in 1988 by eleven European countries. As shown in Figure 1, the facility consists of a 6 GeV storage ring, a full energy injector system and a 200 MeV linear accelerator. Construction of the radiation source from the ground breaking to the start of storage ring commissioning will have taken three years. Subsequently the first set of seven beam lines will be commissioned. They will be fully available for users from 1994 on. Over the following four and a half years, the number of beam lines will be increased to 30.

Construction of the accelerator buildings, the 850 m storage ring tunnel, the annular experimental hall and the utility building started in February 1990. Building activities were scheduled such that the progressive availability of the technical buildings could allow installation and commissioning of the different accelerators in parallel and minimize overlapping of the different activities. Civil works on the central building housing laboratories and offices started early in 1991. The building will be ready by the middle of 1992.

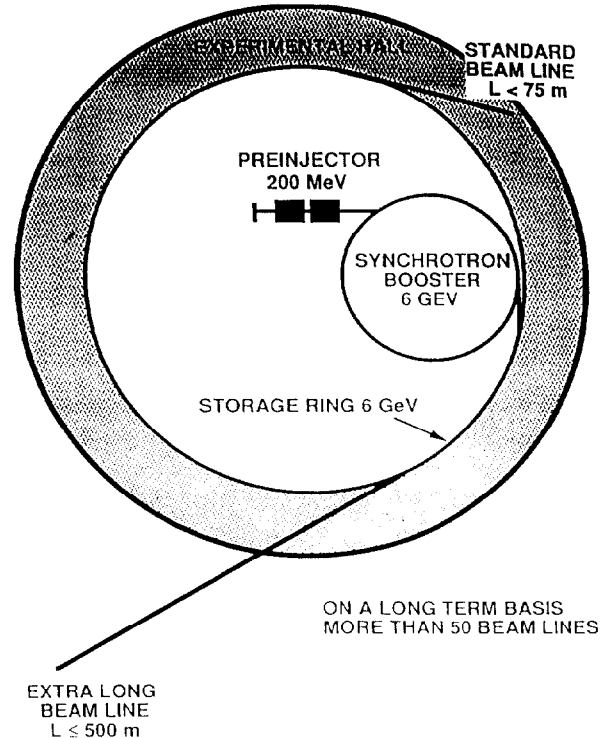


Figure 1. Layout of the ESRF accelerator complex

The preinjector and the synchrotron injector are now operational. Commissioning of the storage ring started in February 1992, with the goal of reaching the target specifications summarized in Table 1 within ten months.

Table 1: Storage ring specifications

Nominal energy	6 GeV	
Emittance	horizontal	$6.9 \cdot 10^{-9}$ m.rad
	vertical	$6.9 \cdot 10^{-10}$ m.rad
Intensity	multibunch	100 mA in 992 bunches
	single bunch	5 mA
Brilliance from undulators	$1.0 \cdot 10^{17}$ phot.s <sup>-1</sup> .mrad <sup>-2</sup> .mm <sup>-2</sup> per 0.1 % bandwidth	
Flux from bending magnets	$8.0 \cdot 10^{12}$ phot.s <sup>-1</sup> .mrad <sup>-1</sup> per 0.1 % bandwidth	
Beam lifetime	$\geq 8$ hours	
Stability	1/10 of dimensions over one shift	

## 2. PREINJECTOR

The 200 MeV electron part of the preinjector was ordered as a turnkey system at the outset of the construction period. Electrons are generated by a 100 kV gun, pass through a prebuncher and a buncher section and are accelerated by two travelling wave sections of 6 m fed by 35 MV klystrons. The linac can be operated in two modes: long pulse mode (1  $\mu$ s) for multibunch operation of the storage ring and short pulse mode (2 ns) for single bunch operation. At the exit of the linac, the beam is transported down to the booster injection septum by a 20 m long transfer line. Most of the diagnostics used to measure the beam characteristics from the linac (current transformer, energy slit selection, wire scanner device for emittance measurement) are installed on the transfer line.

After completion of the factory tests of the major components of the electron linac, installation started in January 1991. The first rough beam was accelerated up to the end of the linac on May 16, 1991. During the following month of commissioning [1], a current of 40 mA was accelerated and design specifications were reached in the 1  $\mu$ s pulse mode ( $I = 25$  mA in  $\Delta E/E = \pm 1\%$ , emittance of  $10^{-8}$  m.rad at 200 MeV). Commissioning of the 2 ns pulse mode was performed in January 1992. The design current is 250 mA (2.5 A in the case of positron operation).

The stability of the electron beam is a key problem for most synchrotron light sources. In the ESRF case, theoretical studies have shown that, at design current and emittance, an electron beam cannot trap ions below mass 50. On the other hand, there is experimental evidence in many places for the presence of dust particles. This cannot be avoided during operation after the first accidental venting. Therefore the ESRF is likely to face trapping of very heavy particles. As far as the addition of a 400 MeV positron linac is concerned, the design study was launched in Autumn 1991 to arrive at the elaboration of technical specifications and a review of the project by Autumn 1992, with possibly some relevant experience from our own machine. Plans are to get prepared to build and commission the positron preinjector before 1994.

## 3. BOOSTER

The booster synchrotron has been designed to ramp the energy from 200 MeV (400 MeV) to 6 GeV. It is operated with a repetition rate of 10 Hz. Focusing of the magnet system is based on a separated function FODO lattice. A three-fold symmetry is created by three dispersion suppression regions used to accommodate the RF cavities, the injection and extraction elements.

Detailed descriptions of the different components are presented at this conference [2], [3], [4]. The main features are outlined here. The quality control of series magnets was performed in the DC mode. Quadrupoles and sextupoles were tested with a rotating coil bench. The dispersion in gradient from one magnet to another is well within specifications ( $\langle \Delta G/G \rangle = 2.0 \cdot 10^{-3}$ ). For the dipoles, a curved coil system traversing a reference magnet and the magnet to be measured was developed. The voltage integrated during the traversal is proportional to the differences in field integral between the two magnets. After magnetic measurements and assignment of the magnets to a given location in the ring according to their magnetic strengths, the half-cell girders with dipole,

quadrupole and sextupole magnets and their thin wall stainless steel vacuum chambers were pre-assembled and pre-aligned outside the tunnel and then transported into the tunnel by special handling equipment.

Magnets are powered by resonant circuits (the so-called "white circuit"). The power converter structure is based on a new technology, using pulse width modulated invertors associated with gate turn off thyristors. The AC and DC power supplies were tested on their load, prior to the start of booster commissioning. Harmonic distortions in the magnetic field of the quadrupoles were found to be induced by the non-linearities of the white chokes. A compensation by modulating the DC power supply at given harmonics has been tried out; it seems that there is no need for it.

The accelerating voltage is provided by two 352.2 MHz five-cell cavities based on the LEP design. Each cavity has two input couplers and two RF windows. The two cavities are powered by an industry built 1 MW transmitter through a circulator and a magic T waveguide system. The RF system has been commissioned in situ to 640 kW peak power which corresponds to nominal operating conditions.

The booster commissioning started on September 2 and was completed in mid December 1991 [5]. The remote control of the main booster components was complete and all the necessary software ready from the start-up of commissioning. For the first turn diagnostics, only eight screens installed along the ring were used, although the 3 GHz detection from the BPM system was operational. On the second day, storage at 200 MeV was successfully achieved without closed orbit correction. Three days later, a beam of 2 mA was accelerated for the first time up to 3 GeV. During the next scheduled commissioning time, further progress was achieved (acceleration to 5 GeV, first extraction tests).

Then in November, a 2 mA beam was accelerated to 6 GeV, extracted and transported downstream the transfer line between the booster and the storage ring. Dedicated diagnostics for closed orbit and tune measurements were used to optimize the transmission during the acceleration cycle (Figure 2). This enabled the betatron tunes to be adjusted to nominal values and the closed orbit at injection to be corrected in both planes down to an amplitude of 4 mm by powering a few steerers in DC. The maximum uncorrected closed orbit at extraction is of the order of 3 mm. These figures show that the magnets are quite well aligned.

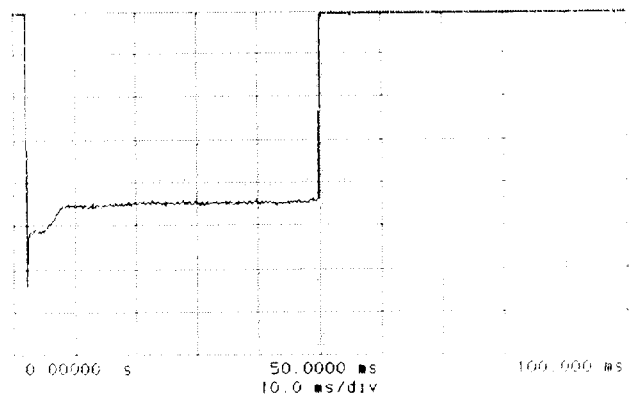


Figure 2. Current during the acceleration cycle from the beam current transformer

However the accelerated current was limited to about 2 mA in the  $\Delta p$ -space by the large natural chromaticity. Also the capture efficiency was not excellent, due to the fact that the RF law was not optimized to compensate for beam loading. In the last two weeks of commissioning, the intensity was boosted to 7.5 mA, which is 50 % above the design figure, and more than 5 mA were extracted into the transfer line. This achievement was possible by powering the chromaticity correcting sextupoles in DC and by adding a frequency modulation of the RF at injection.

#### 4. STORAGE RING

Thanks to the partitioning of the tunnel into four quadrants, installation was able to start as soon as the first quadrant was available. Installation was spread over one year. The construction and the installation of this new generation of ring has implied the use of state-of-the-art techniques in order to achieve the design performances in terms of low emittance, high current and beam lifetime. A certain number of components such as RF (cavities, transmitters and waveguides), magnet measuring devices, beam position monitor system are common to both synchrotron and storage ring. They have benefited from the experience gained during synchrotron installation. However, numerous challenging issues have been raised for most of the equipment.

##### 4.1 Magnets

After field measurements of the prototype magnets had shown that no modifications of pole profile or dimensions were required, except the optimization of the end profile of the quadrupoles, the series manufacture was launched in the second-half of 1990. All magnets were magnetically checked before installation, using the same kind of measuring devices as for the booster [6]. Since the magnets had to be opened afterwards for the installation of vacuum vessels, special care was taken to ensure the reproducibility of their characteristics after this operation. The results of magnetic measurements concerning both the systematic and random components are well within the tolerances imposed by beam optics requirements. The main figures are summarized in Table 2.

Table 2: Storage ring magnets harmonic content

measured	dipole	quadrupole	sextupole
integrated strength	$5.0 \cdot 10^{-4}$	$1.1 \cdot 10^{-3}$	$1.8 \cdot 10^{-3}$
sextupole systematic			
random		$7.0 \cdot 10^{-4}$	
octupole systematic		$1.8 \cdot 10^{-3}$	
random		$1.2 \cdot 10^{-3}$	$3.7 \cdot 10^{-4}$
decapole systematic			
random		$3.4 \cdot 10^{-4}$	$1.6 \cdot 10^{-4}$
12-pole systematic		$1.8 \cdot 10^{-3}$	$4.3 \cdot 10^{-4}$
random		$5.5 \cdot 10^{-4}$	$7.0 \cdot 10^{-4}$
18-pole systematic			$-1.4 \cdot 10^{-4}$
random			$2.4 \cdot 10^{-4}$
30-pole systematic			$-3.3 \cdot 10^{-3}$
random			$2.0 \cdot 10^{-4}$

Although the magnets have been fabricated within tolerances, they have been distributed along the ring according to their magnetic strength. This sorting procedure enables a compensation of defects and therefore less closed orbit and focusing errors. Figure 3 shows a comparison of betatron function modulation after quadrupole sorting and after simulations with random assignment of magnets (dashed areas). The improvement is quite significant.

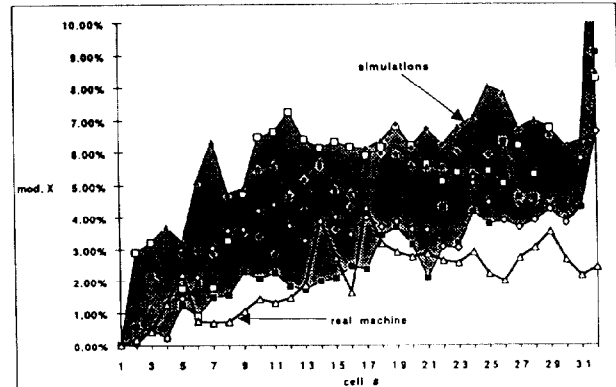


Figure 3. Effect of quadrupole sorting on optics

Each storage ring cell is composed of five girders, two being dipole girders, the other three being quadrupole and sextupole ones. In order to reduce the installation work in the tunnel, a pre-assembly of magnets was performed in the experimental hall. Once the magnets of a given girder had been assigned, they were pre-aligned so that the vacuum chambers could be installed. The upper yoke of the magnets was then opened to insert the vacuum chambers with their bake-out jackets. After closing the magnets, the girder was lifted and pre-aligned in the tunnel, allowing the connection of magnets to their power supplies. A progression rate of one girder per day was achieved during this installation phase.

##### 4.2 Vacuum chambers

These are made from stainless steel with distributed and localized absorbers to absorb the synchrotron radiation. These vessels are sophisticated equipment involving a high level of technology (welding, brazing, tight mechanical tolerances) performed in a very clean environment. The main vessels (dipoles, crotches, bellow-flat absorbers, straight section vessels, beam ports) were constructed by five different suppliers in Europe. Due to the challenging demands, a large effort of supervising the construction of the vessels was made to ensure adequate quality control.

Once the assembly of a sector had been completed, each cell was leak tested and baked in-situ to 200° during a three-day cycle by means of electrical heating tapes. A static pressure in the  $10^{-10}$  mbar range was achieved in all sectors [7]. The residual gas composition was dominated by H<sub>2</sub> (90 %) and H<sub>2</sub>O. The presence of CO, CO<sub>2</sub>, CH<sub>4</sub>, HCl was also detected.

All photon absorbers are made from OFHC copper and are able to sustain the heat load corresponding to the design intensity (100 mA). At the same time, investigations on special copper with improved mechanical properties (Glidcop)

are being carried out to check its outgassing and aptitude to be brazed to stainless steel, so that movable absorbers sustaining a high power density could be changed later on, if required. This is envisaged for upgrading the intensity to 200 mA.

During the design phase, special care was taken to minimize the impedance of the vacuum chamber and to limit the unavoidable cross section changes between different vessels. As far as possible, the cross section ( $70 \times 32 \text{ mm}^2$ ) is kept constant around the circumference. The loss factors of all critical components (flanges, bellows, pumping ports, distributed absorbers, crotches) were checked, using a wire in the centre of the prototype and the well known technique of the synthetic pulse. These controls resulted in the shielding of bellows by special RF fingers, the optimization of dimensions for the grids of pumping ports, the minimization of gap between flanges.

For the installation phase, new wireless methods have been implemented to control the impedance of the vacuum chamber for each cell and to detect possible errors in the assembly [8]. Since the use of the wire method was prohibited by the UHV requirements and the curved geometry of the dipole vessels, waveguide modes were used to detect and localize non-reproducible assemblies. These controls were performed, using both a TM mode transmission method and a waveguide time domain reflectometry method. An example of response of the transmission method is shown in Figure 4.

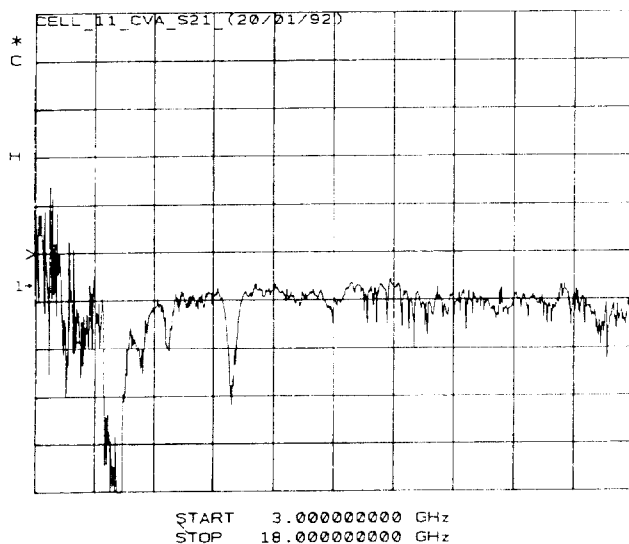


Figure 4. Impedance spectrum

Qualitatively, all the measured cells have a similar dependence on frequency. The larger peak is measured around 8 GHz. This corresponds to a  $Z/p$  for the whole ring smaller than  $0.1 \Omega$ . With the reflectometry method, only small reflections have been observed at the location of crotches, bellows and pumping ports, thus indicating that no severe assembly problem had occurred.

#### 4.3 Alignment and survey ; beam stability

The large amplification of magnet positioning errors by the strong focusing required to achieve a low emittance has imposed tight tolerances on magnet positioning. Alignment

has been performed in two steps: first the magnets on each girder were adjusted with respect to each other within a few tens of microns outside the tunnel; then a general survey of the geodetic network was followed by the final alignment in the tunnel to 0.1 mm [9]. The real-time control of the relative girder vertical position of quadrupoles is performed by means of a hydrostatic levelling system. All the girders are equipped with remote control jacks. This system will allow fast realignments of the machine to compensate for ground settlements.

Short term effects such as those induced by vibrations transmitted through the ground would disturb the beam quality by inducing changes in beam position and a macroscopic emittance growth. A permanent monitoring of the ground vibrations is performed by seismic recording equipment installed in the tunnel. Measurements were performed during installation and compared with early data. They show a small increase of environmental noise. To detect displacements of the beam centre of mass, each insertion device beam line is equipped with X-ray position monitors measuring the photon beam position and angle. This information is transmitted to a feedback steering system that locally corrects the closed orbit deviations. The system will be tested on the machine undulator beam line during commissioning.

#### 4.4 Insertion devices and front-ends

Twenty nine out of the thirty two 6 m long straight sections are available for insertion devices. A segmented approach has been adopted. Each straight section will be equipped with one, two or three segments, each 1.6 m long. The 9 first insertion devices to be installed and commissioned by the end of 1993 are being manufactured [10]. They are characterized by a field ranging from 0.4 to 1.8 T and a gap of 20 mm which was found to be a good compromise between tunability of the insertion devices and safe operation of the machine. Four of the undulator segments have already been measured. The first one, to be used for machine diagnostics purposes, will be installed in mid-1992. In order to ensure the stability of the beam within one tenth of its size when varying the gap of the devices, very severe tolerances have been set on the field integral that must remain below a few  $10^{-5} \text{ T.m}$ . A 2-dimensional shimming procedure has been developed and routinely applied to the first segments to correct these errors.

The strategy adopted for the beam front-ends (high degree of standardization, modular system) has minimized detailed design effort as well as construction and installation time. However, given the difficult problem of heat load (the typical power density is  $25 \text{ kW/mrad}^2$ ), it was necessary to invest in some research and development effort and prototyping before the technical options could be finalized. The front-ends of both bending magnet and insertion device beam lines have been manufactured in two modules equipped with grazing incidence absorbers, vertical slits, two sets of photon position monitors, beryllium windows, fast valves. Most of the seventeen front-ends to be equipped during the first phase have been installed before the start-up of storage ring commissioning.

#### 4.5 First commissioning phase

The commissioning of the storage ring started on schedule

on February 17, 1992. After bringing the injector back to operation, the beam was transmitted over the first turn on February 28. Two days later the first stored beam was obtained. This fast initial turn-on was greatly eased by the fully computer-controlled operation of the machine. According to the specified alignment tolerances on the magnets, there was little chance to get the beam transmitted over the entire circumference from the outset. Therefore the obtention of the first turns circulating in the ring, as soon as the injection parameters were set, must be considered as a significant success.

The beam was injected on-axis with the lattice tuned to the nominal low emittance conditions. It was decided at an early stage of the project that running a detuned lattice in order to reduce the sensitivity to errors would not bring any valuable information. This strategy for commissioning the first third generation ring ever operated proved to be very effective.

The major achievements during this first commissioning phase can be summarized as follows. Amplitudes measured by the BPM system [11] during the first turn transmission were of the order of 15 mm. They were brought down to 4 mm after a careful step by step first turn correction by the closed orbit steerers, thus enabling to get a stored beam after switching on the RF. A 50 - 100 ms lifetime was achieved with sextupoles switched off (see Figure 5). This rather low lifetime was due to the uncorrected chromaticities ( $\xi_x = -115$ ,  $\xi_z = -33$ ) which spread the tune distribution well beyond the neighbouring half integer and integer values. Betatron phase advance measurements were performed on the first turn beam trajectory and allowed to check the focusing.

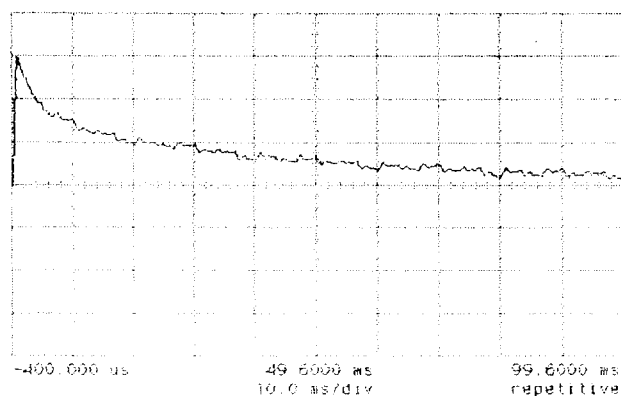


Figure 5. First measurement of lifetime in the storage ring

Commissioning restarted a few days before the Conference. Preliminary results are quite promising: a one hour beam lifetime (limited only by the vacuum) was achieved after switching on the chromaticity sextupoles. The end of the run will be dedicated to first tests of beam accumulation.

During the next commissioning phases, the machine will be tuned to the normal operating mode (off-axis injection, all sextupoles on) and the basic lattice characteristics extensively measured. Although an important milestone has already been reached, there is still much work to be done for bringing the performance to design goals. The emphasis will be put on

closed orbit correction to the 0.1 mm range, stabilization of the beam position with an accuracy of a few microns before increasing progressively the intensity and progressing on vacuum conditioning with beam. Given the present results, there is no reason for these objectives not to be met by the end of 1992.

## 5 CONTROL SYSTEM

The ESRF control system [12] has been operational since August 1991. It is a fully distributed system with computer connections based on the Ethernet standard. The system uses a ring topology based on fiber optics, with four networking centres located around the storage ring tunnel. The system is physically structured as a three layer system. On the lowest level, equipment is interfaced by means of G64 crates. Groups of G64 are connected to multidrop fieldbus that are mastered by group level VME crates. The presentation and process level is made of general server processors and workstations running under UNIX and using the X11 window and Motif standards for the graphics user interface.

Software development was started at an early stage of the project. The low level system software is based on a "client/server" architecture used to distribute software tasks across processors. Server processes are associated with devices and manage all operations on them. In parallel with the implementation of the servers, application programs have been developed by the accelerator physicists. These programs perform basic controls of individual equipment as well as sophisticated procedures involving correction algorithms and elaborate treatment of parameters. Most of them were ready before the start-up of booster commissioning and proved to be a very efficient tool during this phase.

## 6. REFERENCES

- [1] P. Berkvens, "First beam results of the ESRF preinjector", These proceedings
- [2] C. Gough and J.P. Perrine, "Injection and extraction magnets for the ESRF", These proceedings
- [3] J. Jacob et al, "Commissioning and operation of one booster and two storage ring RF acceleration units at the ESRF", These proceedings
- [4] K. Scheidt, "ESRF synchrotron injector beam position monitor system: concept and results", These proceedings
- [5] J.M. Filhol, "ESRF booster synchrotron: characteristics and achieved performance", These proceedings
- [6] M. Lieuvain, A. Ropert and L. Farvacque, "ESRF, the storage ring magnets", These proceedings
- [7] M. Renier, "Vacuum system of the ESRF", These proceedings
- [8] J. Jacob et al, "Wireless impedance measurements and fault location on ESRF vacuum chamber assemblies", These proceedings
- [9] D. Martin, "Survey and alignment", These proceedings
- [10] J. Chavanne et al, "Status of the ESRF insertion devices", These proceedings
- [11] F. Loyer and K. Scheidt, "Project of a beam position monitor for the ESRF storage ring", These proceedings
- [12] W.D. Klotz, "Controlling the ESRF accelerators, status and experiences", These proceedings